Solar powered ROV electric propulsion and control

M. A. Malleswari[1], B. Venkata Rao[2], K. Narasimha Rao[3]
[1]Department of Electrical & Electronics Engineering, GVP College of Engineering (A), Visakhapatnam, India
[2]Electrical Engineering Division, Naval Science and Technological Laboratory, Visakhapatnam, India
[3]Department of Electrical & Electronics Engineering, GVP College of Engineering (A), Visakhapatnam, India
Corresponding author e-mail: malli5695@gmail.com

***Abstract*—Solar powered Remotely Operated Underwater Vehicle (ROV) that is used in the surveillance applications is required to have longer endurance. For achieving this objective the PV based renewable energy is integrated with efficient electric propulsion of the ROV. Since the power generated to be utilized effectively, it is imperative to prefer MPPT techniques. However, for designing optimized ROV propulsion, a combined simulation of ROV propulsion, control and solar power interface is to be done. In this paper, P&O algorithm is used to predict MPP when the dynamics of ROV are integrated with solar simulation. The paper describes the generation & utilization of solar power for different irradiance values with changing depth of the vehicle using MATLAB/SIMULINK® platform. The paper presents the modeling of ROV dynamics integrated to solar output through depth parameter and the maximum power is tracked using P&O algorithm.**

Keywords*—Maximum Power Point Tracking (MPPT); Perturb and Observe (P&O) algorithm; Non-Uniform Illumination (NUI); Gallium Arsenide (GaAs) Photo Voltaic (PV) cell; Pulse Width Modulation (PWM); dynamics of Remotely Operated Underwater Vehicle (ROV); Degrees Of Freedom (DOF)

I. INTRODUCTION

The inexhaustible energy sources became more critical patron and its importance has increased to (20-25)% in recent years [1] for their productivity, pollution-free nature and unwavering quality. Obtaining PV energy from the solar irradiation is one of the enduring technologies as it plays a dominant role in the economic power generation scenario.

The performance of SPV panel is based on the environmental parameters. In order to attain maximum possible power in all instants of time, MPPT algorithms are preferred. The vehicle considered in this paper is a slow moving one and so P&O algorithm is considered to be the simplest method in tracking MPP of the entire MPPT algorithms as it provides flexibility with slow fluctuations during its movement under water [2].

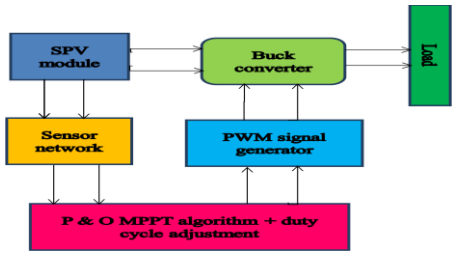

Fig. 1. Block diagram of PV system interfaced with buck converter.

Fig. 1 represents the block diagram of PV system integrated to the load (battery of ROV). The paper focus on P&O algorithm in tracking MPP as the ROV comes to the surface for its battery charging which results in negligible irradiance change. The maximum voltage that is obtained from solar panel using P&O algorithm is reduced using buck converter [3] and is fed to the battery; which after getting charged, powers the vehicle during its motion.

The paper is organized as follows. Section-II presents the mathematical modeling of ROV. Tracking of MPP is presented in section-III. Integration of solar power pack to ROV is discussed in section-IV. The performance is analyzed and the related results from the simulated model are presented in Section-V. In section-VI, the conclusion of the paper is presented and the future scope is discussed in section-VII.

II. MATHEMATICAL MODELLING OF ROV

To understand the dynamic behavior of ROV, it is must to know its sign conventions and its 6 DOF model [4], [5], [6]. The differential equations of motion are developed from the earth fixed and body fixed co-ordinate systems as shown in fig. 2 and is explained by right-handed [7] co-ordinate system.

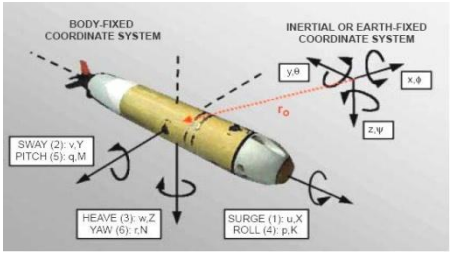

Fig. 2. ROV reference frame

TABLE I. LIST OF PARAMETERS DESCRIBING 6 DOF

DOF	Motion	Forces and moments	Linear and angular velocities	Position and Euler angles
1	Surge	X	U	x
2	Sway	Y	V	y
3	Heave	Z	W	z
4	Roll	K	p	Ø
5	Pitch	M	q	θ
6	Yaw	N	r	ψ

Table 1 presents the 6 DOF motion of the ROV along with their notations.

The position and orientation of ROV [x, y, z, Ø, θ, ψ] are defined in earth fixed frame and the linear and angular velocity components [u, v, w, p, q, r] are defined in body fixed frame.

The motion of ROV is represented by following vectors.

$$\eta = \begin{bmatrix}\eta_1\\ \eta_2\end{bmatrix} \qquad \eta_1 = \begin{bmatrix}x\\ y\\ z\end{bmatrix} = \text{Position vector}$$

$$\eta_2 = \begin{bmatrix}Ø\\ \theta\\ \psi\end{bmatrix} = \text{Euler angle vector} \tag{1}$$

$$\upsilon = \begin{bmatrix}\upsilon_1\\ \upsilon_2\end{bmatrix} \qquad \upsilon_1 = \begin{bmatrix}u\\ v\\ w\end{bmatrix} = \text{Linear velocity vector}$$

$$\upsilon_2 = \begin{bmatrix}p\\ q\\ r\end{bmatrix} = \text{Euler angle vector} \tag{2}$$

$$\tau = \begin{bmatrix}\tau_1\\ \tau_2\end{bmatrix} \qquad \tau_1 = \begin{bmatrix}X\\ Y\\ Z\end{bmatrix} = \text{Force vector}$$

$$\tau_2 = \begin{bmatrix}K\\ M\\ N\end{bmatrix} = \text{Moment vector} \tag{3}$$

The transformation between the two reference co-ordinate systems is determined from eq. (5).

$$J_1(\eta_2) = C^T_{z,\psi} * C^T_{y,\theta} * C^T_{x,Ø}$$

$$= \begin{bmatrix}\cos\psi & -\sin\psi & 0\\ \sin\psi & \cos\psi & 0\\ 0 & 0 & 1\end{bmatrix}\begin{bmatrix}\cos\theta & 0 & \sin\theta\\ 0 & 1 & 0\\ -\sin\theta & 0 & \cos\theta\end{bmatrix}$$

$$\begin{bmatrix}1 & 0 & 0\\ 0 & \cos Ø & -\sin Ø\\ 0 & \sin Ø & \cos Ø\end{bmatrix} \tag{4}$$

$$J_1(\eta_2) =$$

$$\begin{bmatrix}\cos\theta\cos\psi & \sin Ø\sin\theta\cos\psi - \cos Ø\sin\psi & \cos Ø\sin\theta\cos\psi + \sin Ø\sin\psi\\ \cos\theta\sin\psi & \sin Ø\sin\theta\sin\psi + \cos Ø\cos\psi & \cos Ø\sin\theta\sin\psi - \sin Ø\cos\psi\\ -\sin\theta & \sin Ø\cos\theta & \cos Ø\cos\theta\end{bmatrix} \tag{5}$$

The linear velocities in body fixed frame are transformed into position rates in earth fixed frame by using the following transformation.

$$\begin{bmatrix}\dot{x}\\ \dot{y}\\ \dot{z}\end{bmatrix} = J_1(\eta_2)\begin{bmatrix}u\\ v\\ w\end{bmatrix} \tag{6}$$

From eq. (6),

$$\dot{x} = u\cos\theta\cos\psi + v(\sin Ø\sin\theta\cos\psi - \cos Ø\sin\psi) + w(\cos Ø\sin\theta\cos\psi + \sin Ø\sin\psi) \tag{7}$$

$$\dot{y} = u(\cos\theta\sin\psi) + v(\sin Ø\sin\theta\sin\psi + \cos Ø\cos\psi) + w(\cos Ø\sin\theta\sin\psi - \sin Ø\cos\psi) \tag{8}$$

$$\dot{z} = -u\sin\theta + v\sin Ø\cos\theta + w(\cos Ø\cos\theta) \tag{9}$$

The inverse transformation function is given by:

$$\upsilon_1 = J_1^{-1}(\eta_2)\dot{\eta_1} \tag{10}$$

Similarly, the angular velocities in body fixed frame are transformed into Euler rates in earth fixed frame as follows:

$$\dot{Ø} = p + q\sin Ø\tan\theta + r\cos Ø\tan\theta \tag{11}$$

$$\dot{\theta} = q\cos Ø - r\sin Ø \tag{12}$$

$$\dot{\psi} = \frac{q\sin Ø + r\cos Ø}{\cos\theta} \tag{13}$$

Equations (7) to (13) represent the six kinematic equations determining the position rate and Euler rate of ROV. On integrating these rates, we get the trajectory and Euler angles of the vehicle respectively in earth fixed frame as final required outputs.

ROVs are used in different surveillance applications. Application of the vehicle here is to capture the photos of assigned task. For this, different payloads along with propulsion [19] are required with optimal duty of operation and are tabulated as below.

TABLE II. ESTIMATION OF POWER REQUIRED BY DIFFERENT PAYLOADS

Name of the payload	Quantity	Effective power required(W)	Total power required (W)
Thruster [4]	1	9.2	20
Actuator [8]	4	5	
Camera [9]	1	1.92	
MEMS Gyroscope [10]	1	0.5	
Depth transducer [11]	1	2.08	
Antenna [12]	1	1.68	

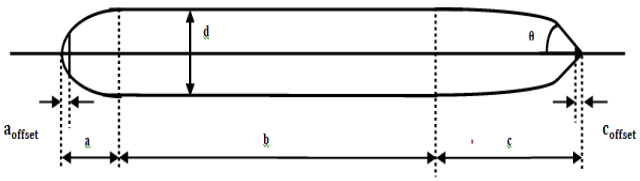

Fig. 3. Dimensions of ROV

Fig. 3 shows the dimensions of vehicle [4] and its parameters are given in table 3.

TABLE III. LIST OF DIMENSIONAL PARAMETERS OF ROV

Parameter	Value	Units	Description
a	+1.91e-001	m	Nose length
a (offset)	+1.65e-002	m	Nose offset
b	+6.54e-001	m	Mid-body length
c	+5.41e-001	m	Tail length
c (offset)	+3.68e-001	m	Tail offset

Diameter of the vehicle (d) = 0.191m and consider the mid–body length (b) of the vehicle to be the effective area for fixing the solar cells i.e., Length of the mid-body of vehicle = 0.7 m

III. TRACKING OF MPP

The area of GaAs PV cell is taken from [13] and the surface area of ROV is determined from [4]. From this data, the designing of solar panel for ROV is done depending on the number of cells that can be arranged on its surface and the electrical characteristics of the solar panel are shown in table 4. The power required by the ROV for its motion and for its in-built payloads is assumed from [4] and [8] to [12].

TABLE IV. ELECTRICAL CHARACTERISTICS OF PV PANEL

Parameter	Value
Open-circuit voltage (V_{OC})	15.4V
Short-circuit current (I_{SC})	1.68A
Maximum voltage (V_{MPP})	13.552V
Maximum current (I_{MPP})	1.603A
Number of cells per module	14
Number of series modules per string	2
Number of parallel strings	7
Maximum power (P_{MPP})	43.45W

The buck converter [3] acts an intermediate source between the source (panel) and the load (battery), which helps in bucking down the voltage level from input to the load side.

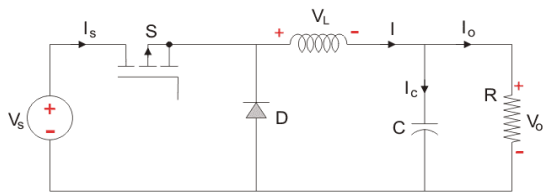

Fig. 4. Typical DC-DC Buck converter

Fig. 4 shows the basic buck converter. Critical value of inductance is calculated by considering,

Voltage across PV panel = voltage across (Inductor + MOSFET + Battery)

Voltage across inductor during ON or OFF switching as

$$v_L = L\frac{di_L}{dt}$$

As switching frequency of PWM generator is 1 KHz, $dt = \frac{1}{2f} = 0.5msec$ and di_L is 85mA.

Current through the dc link capacitor is given by

$$i_C = C\frac{dv_C}{dt}$$

dv_C is 14mV. Finally, the buck converter here is designed with an inductor value of $20e^{-2}$H and a dc link capacitor value of $700e^{-3}$F.

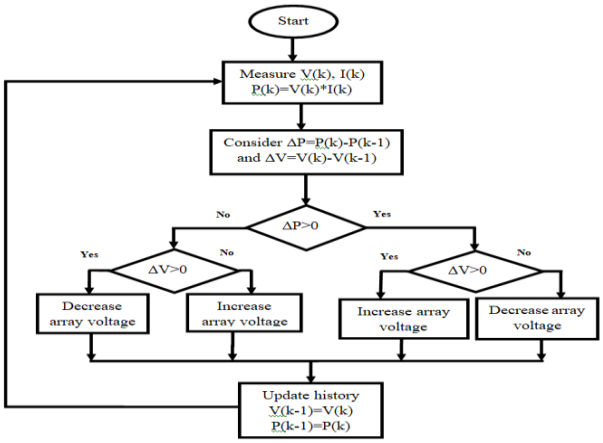

Fig. 5. Flow chart of P&O algorithm

Fig. 5 presents the P&O algorithm [2]. Duty cycle (δ) is increased or decreased depending on panel output, which is examined by varying supply voltage. δ is varied until MPP is reached and the process repeats.

IV. INTEGRATION OF SOLAR POWER PACK TO ROV DYNAMICS

Power required by the vehicle is estimated by considering the amount of effective power that is consumed by the different payloads that are used in the design of ROV. The size of GaAs PV cell is considered from a datasheet reference. Surface area of the vehicle is also calculated to predict the number of cells that can be arranged on to its surface. The V_{OC}, V_{MPP}, I_{SC}, I_{MPP} and finally the maximum power (P_{MPP}) are calculated under standard test conditions i.e., at T = 25^0C and Irr = 1000W/m^2.

In this paper, the variation of irradiation level w.r.t changes in depth is explained and the integration of two simulations is done using the following function.

$$\text{Irr} = \text{fn(D)} = 1000\text{-}(100*\text{D}) \quad (14)$$

Where 1000 is the value of irradiance at STC and is a variable. For different values of depth, the irradiance changes and the corresponding maximum power [15] is delivered to the battery [16] of the ROV.

TABLE V. SPECIFICATIONS OF BATTERY

Parameter	Value
Type	Lithium-Ion
Nominal voltage	12V
Rated capacity	5.4Ah
Initial state-of-charge	10%
Battery response time	0.1s

V. SIMULATED RESULTS

Trajectory of vehicle is resulted from the ROV dynamics. Velocity of vehicle depends on the thrust power required by it [17]. As the vehicle always tends to move in x-direction during its operation, its velocity in y and z-directions is negligible. Velocity of vehicle [4] is 2.38m/s.

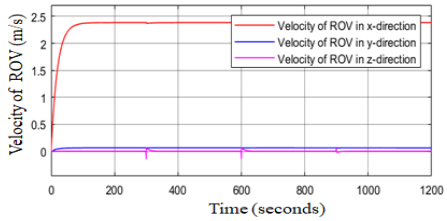

Fig. 6. Velocity of ROV in x,y,z axes respectively

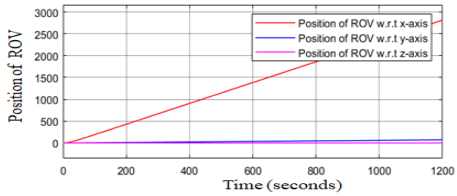

Fig. 7. Position of ROV in x,y,z axes respectively

Fig. 6 and fig. 7 show the velocity and position of ROV with respect to their respective axes.

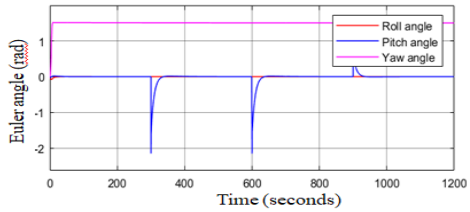

Fig. 8. Euler angles

Fig. 8 shows the orientation of vehicle. As the vehicle is pre - programmed, the commands are given initially. It was programmed that the roll angle must be zero after certain disturbances. And it is also programmed to make a yaw angle of 1.5rad. The pitch is dependent on the depth of the vehicle. After the depth gets settled to a determined value, the pitch sets itself to zero.

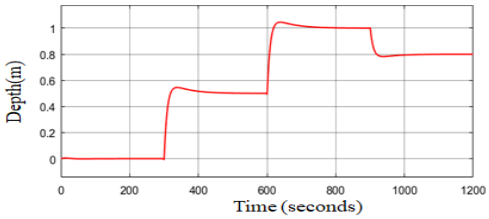

Fig. 9. Motion of the ROV w.r.t depth

Fig. 9 represents the motion of the vehicle w.r.t to depth. The graph shows how the ROV gets settled to the different depth values of 0m, 0.5m, 1m and 0.8m.

In this methodology, the variation in maximum power generation w.r.t change in irradiance as a change of depth parameter of simulated ROV dynamics is presented.

TABLE VI. MPP AT IRRADIANCE = 1000 WATTS PER SQUARE METER

Depth (m)	Irradiation (W/m^2)	Input Power(W)	Output Power(W)
0	1000	43.45	41.86
0.5	800	34.6	33.49
0.8	680	29.33	28.53
1	600	25.77	25.14

The following are the simulated graphs at input side for irradiance = 1000 W/m^2

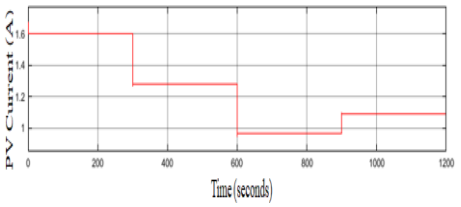

Fig. 10. PV Current at 1000 W/m^2

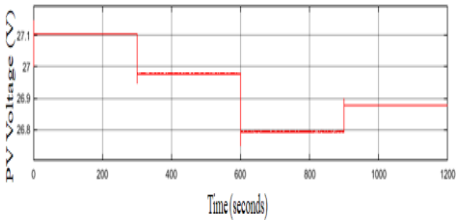

Fig. 11. PV Voltage at 1000 W/m^2

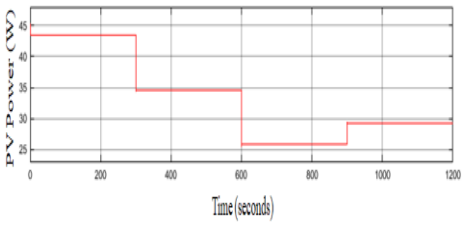

Fig. 12. PV Power at 1000 W/m^2

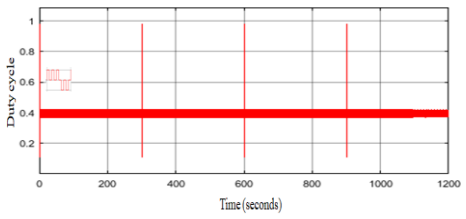

Fig. 13. Duty Cycle at 1000 W/m^2

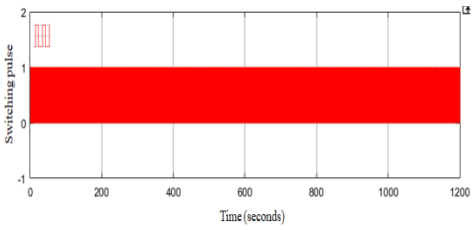

Fig. 14. Switching pulses to the buck converter at 1000 W/m^2

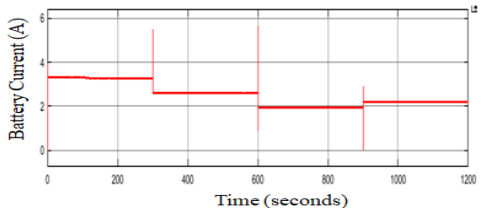

Fig. 15. Battery Current at 1000 W/m^2

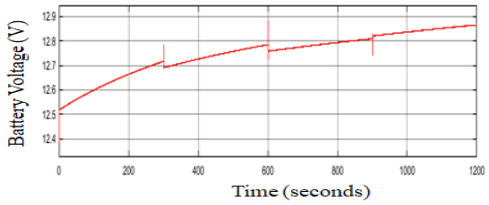

Fig. 16. Battery Voltage at 1000 W/m^2

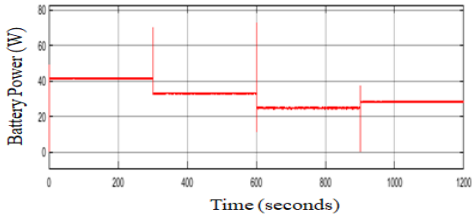

Fig. 17. Battery Power at 1000 W/m^2

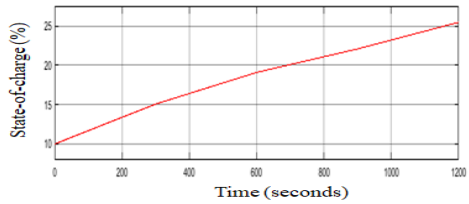

Fig. 18. State-of-charge at 1000 W/m^2

Fig. 13 and fig. 14 are the simulated graphs of inputs to the buck converter and fig. 15 to fig. 18 are the simulated graphs at output side for irradiance = 1000 W/m^2.

Similarly, the maximum power values at two different irradiations on 31st March, 2014 [18] i.e., at 958 W/m^2 and at 873 W/m^2 are also obtained for the depth values of 0m, 0.5m, 1m and 0.8m respectively where 958 is the highest value of irradiance on the considered day.

TABLE VII. MPP AT IRRADIANCE = 958WATTS PER SQUARE METER

Depth (m)	Irradiation (W/m^2)	Input Power(W)	Output Power(W)
0	958	41.59	40.09
0.5	758	32.74	31.72
1	558	23.92	23.88
0.8	638	27.44	26.66

The following are the simulated graphs at input side for irradiance = 958W/m^2

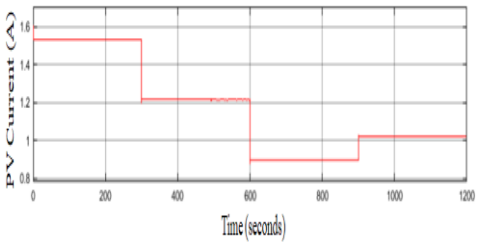

Fig. 19. PV Current at 958 W/m^2

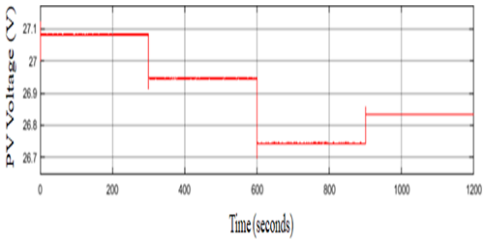

Fig. 20. PV Voltage at 958 W/m^2

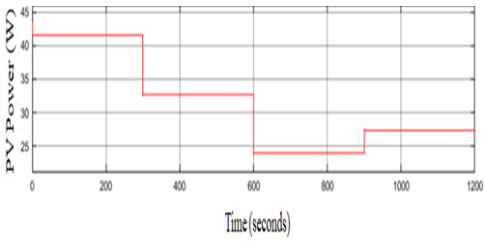

Fig. 21. PV Power at 958 W/m^2

The duty cycle varies between 0.35 and 0.44 as there is minor change in considered irradiation levels the following are the simulated graphs at output side at 958 W/m^2.

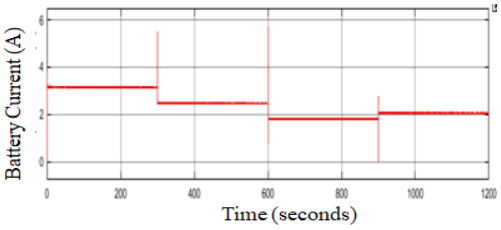

Fig. 22. Battery Current at 958 W/m^2

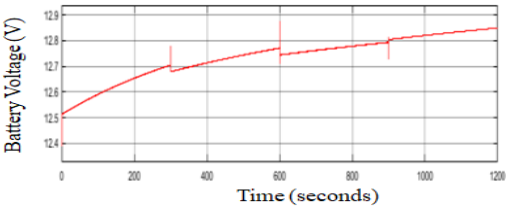

Fig. 23. Battery Voltage at 958 W/m^2

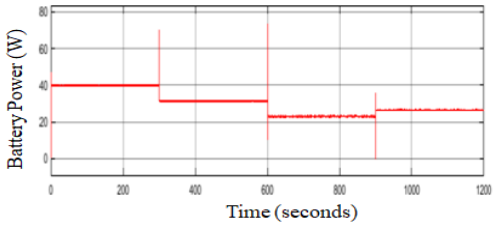

Fig. 24. Battery Power at 958 W/m^2

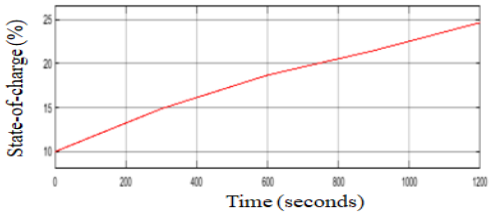

Fig. 25. State-of-charge at 958 W/m^2

TABLE VIII. MPP AT IRRADIANCE = 873WATTS PER SQUARE METER

Depth (m)	Irradiation (W/m^2)	Input Power(W)	Output Power(W)
0	873	37.83	36.57
0.5	673	28.99	28.16
1	473	20.19	19.84
0.8	553	23.7	23.6

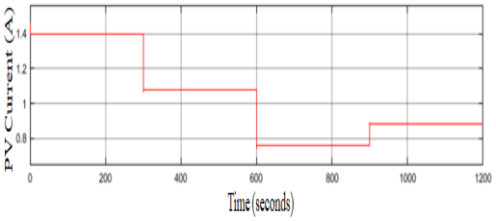

Fig. 26. PV Current at 873W/m^2

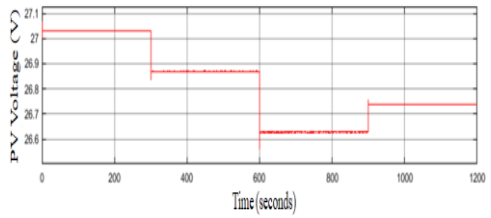

Fig. 27. PV Voltage at 873 W/m^2

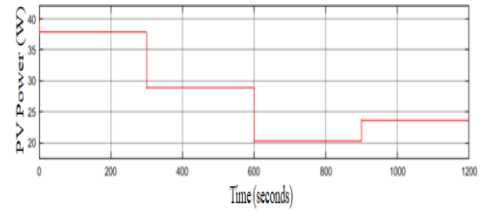

Fig. 28. PV Power at 873 W/m^2

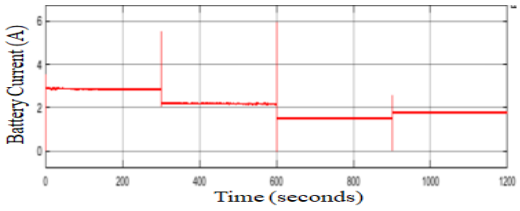

Fig. 29. Battery Current at 873 W/m^2

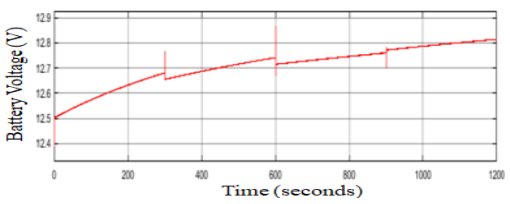

Fig. 30. Battery Voltage at 873 W/m^2

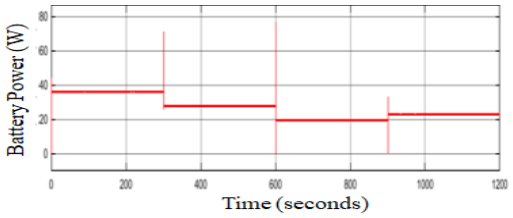

Fig. 31. Battery Power at 873 W/m^2

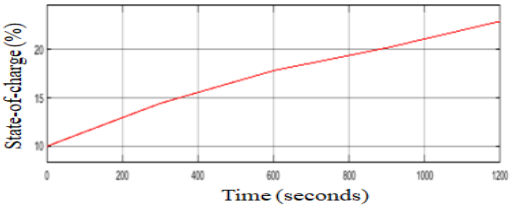

Fig. 32. State-of-charge at 873 W/m^2

From fig. 18, it is clear that the battery takes 1hr 56 min to get charged at 1000W/m2. Similarly, it takes 2hrs 3 min at 958W/m2 and 2hr 19 min at 873W/m2 for its complete charging. As the ROV require 20W, current through the load will be 1.6A. If the battery is charged to 100%, then the vehicle can work upto (5.4/1.6) hrs i.e., upto 3 hrs 22 min 5 sec.

VI. CONCLUSION

The paper presents the idea of how the change in depth of a vehicle causes a change in maximum power generation from the panel. Design of solar panel in simulation is done in general as the required parameters like number of cells per module; its open circuit voltage, short circuit currents and their temperature coefficients; number of series connected modules per string and number of parallel strings of the complete array can be given easily. It is requisite to generate maximum possible power and this is done using the P&O algorithm as this algorithm possess a soft behavior, which extends the valuable life span of power electronic devices. Also, the P&O algorithm has the desirable adaptability to slowly fluctuating solar irradiation, temperature, and even variation of the PV panels.

By adjusting the PWM duty to the power converter, maximum power is obtained. Both the ROV dynamics and the solar simulation with P&O technique are integrated using MATLAB/SIMULINK® software. This paper explains how the maximum power is generated to run the vehicle and how it varies with the change in depth.

VII. FUTURE SCOPE

Depth is one of the parameters of ROV dynamics. Along with this parameter, there are other parameters like roll, pitch and yaw. Currently, in this paper, integration of solar power pack with ROV dynamics as a function of depth is presented. There is a future scope in which NSTL team would work on all the remaining parameters with efficient MPPT techniques.

VIII. ACKNOWLEDGEMENTS

The authors would acknowledge the Naval Science and Technological Laboratory (NSTL) team for their support and research facilities.

REFERENCES

[1] R. T. Ahmad Hamdi, "Solar cell system simulation using Matlab-Simulink", *Kurdistan J. Appl. Res.*, vol. 2, no. 1, pp. 45-51, June 2017.

[2] L. S. Chaitanya Kumar, K. Padma, "Matlab/Simulink based modelling and simulation of residential grid connected solar photovoltaic system", *Int. J. Eng. Res. Technol.*, vol. 3, no. 3, pp. 1577-1586, Mar. 2014.

[3] A. Satif, L. Hlou, M. Benbrahim, H. Erguig and R.Elgouri, "Simulation and analysis of a PV system with P and O MPPT algorithm using a PI controller for Buck converter", *ARPN J. Eng. Appl. Sci.*, vol. 13, no. 9, pp. 3014-3022, May 2018.

[4] T. Prestero, "Verification of a six-degree of freedom simulation model for the REMUS autonomous underwater vehicle", *Master's thesis, B.S. Mech. Eng., Univ. of California at Davis*, Sep. 2001.

[5] O. A. Aguirre-Castro *et al.*, "Design and construction of an ROV for underwater exploration", *MDPI, Sensors (Switzerland)*, vol. 19, no. 24, pp. 1-25, Dec. 2019.

[6] A. Manzanilla, S. Reyes, M. Garcia, D. Mercado and R. Lozano, "Autonomous navigation for unmanned underwater vehicles: Real-time experiments using computer vision", *IEEE Robot. Autom. Lett.*, vol. 4, no. 2, pp. 1351-1356, Apr. 2019.

[7] W. Rustrian, "Modeling of a small Remotely Operated underwater Vehicle for autonomous navigation and control", *M. S. in Mech. Eng., California State Univ., Long Beach*, May 2016.

[8] URL:http://heating.danfoss.com/PCMPDF/VDLFO202_AMB162-182.pdf

[9] URL:http://www.penguin.cz/~utx/hardware/USB_Camera_AX2311/PDS-Family-USB-cameras.pdf

[10] URL:https://www.st.com/resource/en/datasheet/a3g4250d.pdf

[11] URL:https://www.iongeo.com/content/documents/Resource%20Center/Brochures%20and%20Data%20Sheets/Data%20Sheets/Marine%20Systems/Source%20and%20Source%20Control/DS_MIS_Pressure_Transducer.pdf

[12] URL:https://www.navico-commercial.com/Root/SimradProSeries_docs/SIMRAD_MX521A_PROD_SHEET.pdf

[13] URL:http://www.altadevices.com/wp-content/uploads/2018/04/Single-Junction-Tech-Brief.pdf

[14] J. J. Nedumgatt, K. B. Jayakrishnan, S. Umashankar, D. Vijayakumar, D. P. Kothari, "Perturb and observe MPPT algorithm for solar PV systems-modeling and simulation", *Annu. IEEE India Conf. Eng. Sustain. Solut. INDICON-2011*, vol. 19, no. 1, pp. 1-6, 2011.

[15] S. M. Gupta and A. R. Saxena, "Analysis of Perturb & Observe MPPT algorithm for PV system interfaced with Boost converter under changing climatic conditions", *Int. J. Curr. Eng. Technol.*, vol. 4, no. 3, pp. 2189-2195, June 2014.

[16] A. Rana, S. Gian, M. Kumar, "Solar power mobile charger using Buck converter", *B. Tech. Project report, Dept. of Elec. Eng., RCC Institute of Inf. Technol.* 2018.

[17] M. P. R. Prasad & A. Swarup, "Position and velocity control of Remotely Operated underwater Vehicle using model predictive control", *Indian J. Geo-Marine Sci.*, vol. 44, no. 12, pp. 1920-1927, Dec. 2015.

[18] URL:https://maps.nrel.gov/nsrdb-viewer/

[19] G. Martos, A. Abreu, S. Gonzalez, "Remotely Operated underwater Vehicle (ROV)", *B. Sc. Thesis, B.S. Mech. Eng., Florida Int. Univ.*, Sep. 2013.